

## *N, N*-dimethyltryptamine forms oxygenated metabolites via CYP2D6 - an *in vitro* investigation

Emma Eckernäs, Alicia Macan-Schönleben, Moa Andresen-Bergström, Sofia Birgersson, Kurt-Jürgen Hoffmann & Michael Ashton

To cite this article: Emma Eckernäs, Alicia Macan-Schönleben, Moa Andresen-Bergström, Sofia Birgersson, Kurt-Jürgen Hoffmann & Michael Ashton (2023) *N, N*-dimethyltryptamine forms oxygenated metabolites via CYP2D6 - an *in vitro* investigation, *Xenobiotica*, 53:8-9, 515-522, DOI: [10.1080/00498254.2023.2278488](https://doi.org/10.1080/00498254.2023.2278488)

To link to this article: <https://doi.org/10.1080/00498254.2023.2278488>



© 2023 The Author(s). Published by Informa UK Limited, trading as Taylor & Francis Group.



View supplementary material [↗](#)



Published online: 26 Nov 2023.



Submit your article to this journal [↗](#)



Article views: 401



View related articles [↗](#)



View Crossmark data [↗](#)

RESEARCH ARTICLE



## *N*, *N*-dimethyltryptamine forms oxygenated metabolites via CYP2D6 - an *in vitro* investigation

Emma Eckernäs<sup>a</sup>, Alicia Macan-Schönleben<sup>b</sup>, Moa Andresen-Bergström<sup>c,d</sup>, Sofia Birgersson<sup>a</sup>, Kurt-Jürgen Hoffmann<sup>a</sup> and Michael Ashton<sup>a</sup>

<sup>a</sup>Unit for Pharmacokinetics and Drug Metabolism, Department of Pharmacology, Sahlgrenska Academy at University of Gothenburg, Gothenburg, Sweden; <sup>b</sup>Toxicological Centre, University of Antwerp, Wilrijk, Belgium; <sup>c</sup>Laboratory of Clinical Chemistry, Sahlgrenska University Hospital, Gothenburg, Sweden; <sup>d</sup>Department of Laboratory Medicine, Institute of Biomedicine, Sahlgrenska Academy, University of Gothenburg, Gothenburg, Sweden

### ABSTRACT

1. *N*, *N*-dimethyltryptamine (DMT) is a psychedelic compound that has shown potential in the treatment of depression. Aside from the primary role of monoamine oxidase A (MAO-A) in DMT metabolism, the metabolic pathways are poorly understood. Increasing this understanding is an essential aspect of ensuring safe and efficacious use of DMT.
2. This work aimed to investigate the cytochrome 450 (CYP) mediated metabolism of DMT by incubating DMT with recombinant human CYP enzymes and human liver microsomes (HLM) followed by analysis using high-resolution mass spectrometry for metabolite identification.
3. DMT was rapidly metabolised by CYP2D6, while stable with all other investigated CYP enzymes. The metabolism of DMT in HLM was reduced after inclusion of harmine and SKF-525A whereas quinidine did not affect the metabolic rate, likely due to MAO-A residues present in HLM. Analysis of the CYP2D6 incubates showed formation of mono-, di- and tri-oxygenated metabolites, likely as a result of hydroxylation on the indole core.
4. More research is needed to investigate the role of this metabolic pathway *in vivo* and any pharmacological activity of the proposed metabolites. Our findings may impact on safety issues following intake of ayahuasca in slow CYP2D6 metabolizers or with concomitant use of CYP2D6 inhibitors.

### ARTICLE HISTORY

Received 7 September 2023  
Revised 29 October 2023  
Accepted 30 October 2023

### KEYWORDS

*N* *N*-dimethyltryptamine; DMT; cytochrome P450; human liver microsomes; *in vitro* metabolism


### Introduction

*N*, *N*-dimethyltryptamine (DMT) is a psychedelic compound that is naturally occurring in a variety of plants. It is the active ingredient in the traditional Amazonian brew ayahuasca, which also contains harmala alkaloids such as harmine, harmaline and tetrahydroharmine (Dobkin de Rios 1971). In recent years, DMT/ayahuasca has gained increased attention, as it has been shown to reduce symptoms in patients suffering from severe depression (Sanches et al. 2016; Palhano-Fontes et al. 2019; D'Souza et al. 2022). Consequently, there is increasing research ongoing aimed at investigating DMT as a potential future therapeutic option in mental disorders. However, aside from studying the therapeutic benefits, much remains to be known about the disposition of DMT in the human body before it can be safely administered in a wider population. This includes having a detailed understanding of the metabolic pathways and the contribution of different enzymes to the drug's disposition in

order to understand the risk for potential drug-drug interactions (Food and Drug Administration 2020).

While the primary role of monoamine oxidase A (MAO-A) in DMT metabolism is well established, it is not clear which other enzymes may be involved. Furthermore, the metabolic pattern of DMT appears to shift depending on the method of administration. When DMT is administered orally alone, it is not active due to extensive first pass metabolism (Riba et al. 2015). This metabolism is primarily mediated by MAO-A resulting in formation of the inactive metabolite indole 3-acetic acid (IAA) (Riba et al. 2012). After intravenous administration of DMT alone, IAA is the only metabolite that has been measured in any substantial amount, while lesser amounts of DMT *N*-oxide (DMT-NO) have also been observed (Eckernäs et al. 2022; Luethi et al. 2022; Vogt et al. 2023). However, when administered orally as ayahuasca, the harmala alkaloids act as MAO-A inhibitors enabling DMT to reach the systemic circulation without a significant first-pass

**CONTACT** Emma Eckernäs  [emma.eckernas@gu.se](mailto:emma.eckernas@gu.se)  Unit for Pharmacokinetics and Drug Metabolism, Sahlgrenska Academy, University of Gothenburg, Box 431, 405 30 Gothenburg, Sweden

 Supplemental data for this article can be accessed online at <https://doi.org/10.1080/00498254.2023.2278488>.

© 2023 The Author(s). Published by Informa UK Limited, trading as Taylor & Francis Group.  
This is an Open Access article distributed under the terms of the Creative Commons Attribution License (<http://creativecommons.org/licenses/by/4.0/>), which permits unrestricted use, distribution, and reproduction in any medium, provided the original work is properly cited. The terms on which this article has been published allow the posting of the Accepted Manuscript in a repository by the author(s) or with their consent.

metabolism (Buckholtz and Boggan 1977). After administration of ayahuasca, several metabolites of DMT have been observed in urine and plasma, with IAA being the most prominent, followed by DMT-NO (McIlhenny et al. 2012; Riba et al. 2012). Lesser amounts of the demethylated product *N*-methyltryptamine (NMT) as well as a hydroxylated product have also been reported (Szara and Axelrod 1959; Riba et al. 2012). After smoking of DMT, a decrease in conversion to IAA has been observed and an increase in formation of DMT-NO, as compared to after oral intake of DMT alone (Riba et al. 2015). A recent *in vitro* investigation showed that DMT is a substrate for the cytochrome P450 (CYP) enzymes CYP2D6 and CYP2C19 (Good et al. 2023). However, no metabolite profiling or identification data was presented.

Currently, the metabolic pathways of DMT are not fully understood. Furthermore, while several potential metabolites have been identified after administration of ayahuasca, the complexity of the ayahuasca brew makes it difficult to conclude which metabolites are formed specifically from DMT. No human *in vivo* metabolic profiling has been performed and there may still be unidentified metabolites.

To increase the understanding of DMT metabolism, the aim of this work was to further study the role of CYP enzymes in the metabolism of DMT *in vitro* and to investigate which metabolites are formed *via* these enzymes. This was conducted using human liver microsomes (HLM) as well as recombinant CYP enzymes.

## Methods and materials

### Materials

DMT hemifumarate, DMT-NO, 5-hydroxy DMT (bufotenine) and 4-hydroxy DMT (psilocin) were purchased from Chiron AS (Trondheim, Norway). NMT, SKF-525A, quinidine and harmine were purchased from Sigma Aldrich (St. Louis, MO, USA). Deuterated *N*, *N*-dimethyltryptamine (DMT-D<sub>6</sub>) was purchased from Toronto Research Chemicals (North York, ON, Canada). IAA and 2-methyl-indole 3-acetic acid (Me-2 IAA) were purchased from Alfa Aesar (Kandel, Germany). Na<sub>2</sub>HPO<sub>4</sub> was purchased from Scherlau (Steinheim, Germany) and NaH<sub>2</sub>PO<sub>4</sub> from Fluka (Barcelona, Spain). Formic acid (FA), LC-MS grade methanol and acetonitrile (ACN) were purchased from Fisher Scientific (Hampton, NH, USA). Water was deionised by a Milli-Q system (Millipore, Burlington, MA, USA). HLM pooled from 150 donors (both male and female), recombinant CYP isoforms (CYP1A2, CYP2A6, CYP2B6, CYP2C8, CYP2C9, CYP2C19, CYP2D6, CYP2E1, CYP3A4, CYP3A5) expressed in baculovirus-transfected insect cells, NADPH generating solutions and negative controls prepared from insect cells were purchased from Corning (Woburn, MA, USA). All experiments were performed using 1.5 mL SafeSeal polypropylene tubes purchased from Sarstedt AG & Co.KG (Nümbrecht, Germany)

### Preparation of stock and working solutions

Stock solutions of all compounds were prepared in methanol and stored at  $-20^{\circ}\text{C}$ . Stock solutions were prepared at the

following concentrations; DMT 150  $\mu\text{M}$ , IAA 1 mM, DMT-NO 100  $\mu\text{M}$ , quinidine 10 mM, harmine 10 mM, SKF-525 A 10 mM, psilocin 1 mM, bufotenine 100  $\mu\text{M}$ . Working solutions were prepared fresh daily by diluting stock solutions of each analyte with water to the appropriate concentrations.

### Incubations with recombinant CYP enzymes

To investigate the involvement of CYP enzymes in DMT metabolism, DMT (1  $\mu\text{M}$ ) was incubated with each CYP isoenzyme (20 nM) and an NADPH regenerating system (2.6 mM NADP<sup>+</sup>, 6.6 mM glucose-6-phosphate, 6.6 mM MgCl<sub>2</sub> and 4 U/mL glucose 6-phosphate dehydrogenase) in phosphate buffer (100 mM, pH 7.4) at a final volume of 1 mL. Samples were pre-incubated at 37  $^{\circ}\text{C}$  for 5 min before the reaction was initiated by addition of enzyme. Incubations proceeded at 37  $^{\circ}\text{C}$  for 60 min and aliquots of 100  $\mu\text{L}$  were removed at 0 (before the reaction was initiated), 5, 10, 20, 30 and 60 min. Reactions were quenched by addition of ice-cold acetonitrile (300  $\mu\text{L}$ ) spiked with DMT-D<sub>6</sub> (100 nM) and 2-Me-IAA (300 nM) as internal standards. Samples were centrifuged at 10,000  $\times g$  for 2 min, supernatants were transferred into new vials and were either analysed directly or stored at  $-80^{\circ}\text{C}$  before analysis. Experiments were performed in duplicates.

DMT half-life was calculated by log-linear regression of the terminal decline of DMT concentrations using Microsoft Excel (Microsoft Corporation; Redmond, WA, U.S.).

### Inhibition of CYP enzymes in HLM

To further assess the contribution of specific CYP enzymes to DMT metabolism, DMT (1  $\mu\text{M}$ ) was incubated with HLM (0.5 mg/mL) and an NADPH regenerating system (1.3 mM NADP<sup>+</sup> + 3.3 mM Glucose-6-phosphatase + 3.3 mM magnesium chloride, 0.4 U/mL glucose-6-phosphate dehydrogenase) in phosphate buffer (100 mM, pH 7.4) in the presence or absence of quinidine (a CYP2D6 inhibitor), harmine (inhibitor of MAO-A and CYP2D6) or SKF-525A (a general CYP inhibitor) at a total volume of 1 mL. Samples were pre-incubated at 37  $^{\circ}\text{C}$  for 5 min before the reaction was initiated by addition of HLM. Incubations proceeded at 37  $^{\circ}\text{C}$  for 60 min and aliquots of 100  $\mu\text{L}$  were removed at 0 (before the reaction was initiated), 5, 10, 20, 30 and 60 min. Reactions were quenched by addition of ice-cold acetonitrile (300  $\mu\text{L}$ ) spiked with the internal standards DMT-D<sub>6</sub> (100 nM) and 2-Me-IAA (300 nM). Samples were centrifuged at 10,000  $\times g$  for 2 min, supernatants were transferred into new vials and were either analysed directly or stored at  $-80^{\circ}\text{C}$  before analysis. Experiments were performed in duplicates. DMT half-life was calculated in the same way as for the incubations with recombinant CYP enzymes.

### Quantitative analysis by LC-MS/MS

Samples were analysed for presence of DMT, IAA and DMT-NO using a previously published liquid chromatography tandem mass spectrometry (LC-MS/MS) method (Eckernäs et al. 2022). In brief, multiple reaction monitoring was performed

with an API 4000 triple quadrupole mass spectrometer (AB Sciex, Framingham, MA, USA) operated in positive ion mode. Analytes were separated on a SpeedCore Diphenyl column (50 × 2.1 mm, 2.6 μm, Fortis Technologies Ltd, Cheshire, UK) with gradient elution using water with 0.1% formic acid as mobile phase A and methanol with 0.1% formic acid as mobile phase B. The gradient program was initiated with a 2 min hold at 5% mobile phase B followed by a linear ramp over 1 min to 95% mobile phase B and a 2 min hold. This was followed by a linear decrease to 5% mobile phase B over 1 min and a final re-equilibration step at 5% mobile phase B for 2 min before injection of the next sample. Injection volume was 10 μL and mobile phase flow rate 0.4 mL/min. Data acquisition and processing was performed in Analyst 1.6.3 (AB Sciex, Framingham, MA, USA).

Calibration standards were prepared by diluting working solutions of each analyte in 1:3 phosphate buffer:acetonitrile spiked with the internal standards. Nine-point calibration curves were constructed with the concentrations of all analytes being 0.25, 5, 20, 75, 100, 125, 175, 200 and 250 nM. Quality control samples, prepared in the same way as calibration standards but from separate stock solutions at 10, 110 and 220 nM, were analysed in duplicates on each experimental occasion. Quantitation was considered acceptable if accuracy was within ±15% of nominal concentration.

### Metabolite identification with LC-HRMS

After incubating DMT with HLM and CYP2D6, samples were further analysed to screen for unidentified metabolites. Analysis was performed using a Waters Aquity I-class ultra-performance liquid chromatography (UPLC) system coupled to a Vion ion-mobility spectrometry (IMS)-quadrupole time-of-flight tandem mass spectrometer (Waters Corporation) equipped with an electrospray interface. Analytes were separated on a Waters Acquity UPLC HSS T3 analytical column (2.1 × 150 mm, 1.8 μm particle size). An injection volume of 1 μL was used at a flow rate of 0.4 mL/min. Mobile phase A consisted of 5 mM ammonium formate and 0.1% formic acid in water and mobile phase B of 0.1% formic acid in acetonitrile. A linear gradient of 2–15% B over 15 min was followed by a second gradient of 15–95% B over 0.5 min and ended in isocratic elution at 95% B for 2 min. The column was equilibrated at 2% B for 2.2 min before the next injection. Positive electrospray ionisation mode was used with capillary and cone voltages of 0.3 kV and 30 V, respectively. The source and desolvation temperatures were 150 °C and 550 °C, and the cone and desolvation gas flows were 20 and 600 L/h, respectively. MS data were acquired in MS<sup>E</sup> mode, a data-independent acquisition mode which uses alternating high and low collision energies for collection of full-scan data. The scan range was m/z 50–800 and the scan time was 0.15 s. A collision energy of 6 eV was applied during the low energy phase and a ramp of 28–56 eV during the high energy phase, with nitrogen as collision gas. Product ion scans (MSMS) were acquired for detected major metabolites using a precursor ion window of approximately 1 Da, a product ion scan range of m/z 50–300 and fixed collision energies

of 10, 20 or 30 eV. The Waters UNIFI software v 3.1 was used for data acquisition and processing. Metabolites were detected using accurate mass screening of MS<sup>E</sup> data and transformation generation within the Waters UNIFI software. The software automatically searched for selected phase I metabolites and cleaved metabolites. All tentative metabolites with a mass accuracy <5 ppm and a response over 300 were considered.

## Results

### CYP enzymes involved in DMT metabolism

After incubation of DMT with ten different CYP isoforms, only CYP2D6 was shown to metabolise DMT to any significant extent, with a DMT half-life of 10.5 min. DMT was stable in the incubations with CYP1A2, CYP2A6, CYP2B6, CYP2C8, CYP2C9, CYP2C19, CYP2E1, CYP3A4 or CYP3A5. IAA or DMT-NO were not detected in any of the incubations.

### Metabolic stability of DMT in human liver microsomes

After incubation of DMT with HLM, DMT was rapidly metabolised with substantial amounts of IAA formed. No DMT-NO could be detected. When co-incubated with harmine (an inhibitor of both MAO-A and CYP2D6), DMT metabolism was completely inhibited. Co-incubation with the CYP2D6 specific inhibitor quinidine did not appear to affect DMT disappearance to any substantial degree. The general CYP inhibitor SKF-525A had a larger impact on DMT metabolism compared to quinidine (2.1-fold increase in half-life). Results are summarised in Table 1.

### Metabolite identification

After incubation of DMT with CYP2D6, four major metabolites were detected and denoted as M1–M4 according to ascending retention time (Table 2). The metabolic pattern changed over time (Figure 1) with the mono-oxygenated metabolite M4 being the dominant peak at early time points.

**Table 1.** Average half-life of DMT after incubation with human liver microsomes in the absence or presence of different enzyme inhibitors.

Inhibitor	Half-life (min)
No inhibitor	11.3
Harmine	NA
Quinidine	11.6
SKF-525A	24.2

Harmine: MAO-A inhibitor; Quinidine: CYP2D6 inhibitor; SKF-525A: general CYP-enzyme inhibitor; NA: not applicable

**Table 2.** Proposed formula, transformation, retention time (RT), mass of molecular ion and mass error (ppm) of DMT and metabolites after incubation with CYP2D6.

ID	Proposed formula	Transformation	RT (min)	m/z	ppm
M1	C <sub>12</sub> H <sub>16</sub> N <sub>2</sub> O <sub>3</sub>	Tri-oxygenation (+3 O)	1.30	237.1230	−1.4
M2	C <sub>12</sub> H <sub>16</sub> N <sub>2</sub> O <sub>2</sub>	Di-oxygenation (+2 O)	3.25	221.1281	−1.5
M3	C <sub>12</sub> H <sub>16</sub> N <sub>2</sub> O <sub>2</sub>	Di-oxygenation (+2 O)	3.42	221.1281	−1.5
M4	C <sub>12</sub> H <sub>16</sub> N <sub>2</sub> O	Oxygenation (+O)	4.26	205.1329	−3.0
DMT	C <sub>12</sub> H <sub>16</sub> N <sub>2</sub>	–	9.37	189.1384	−1.2

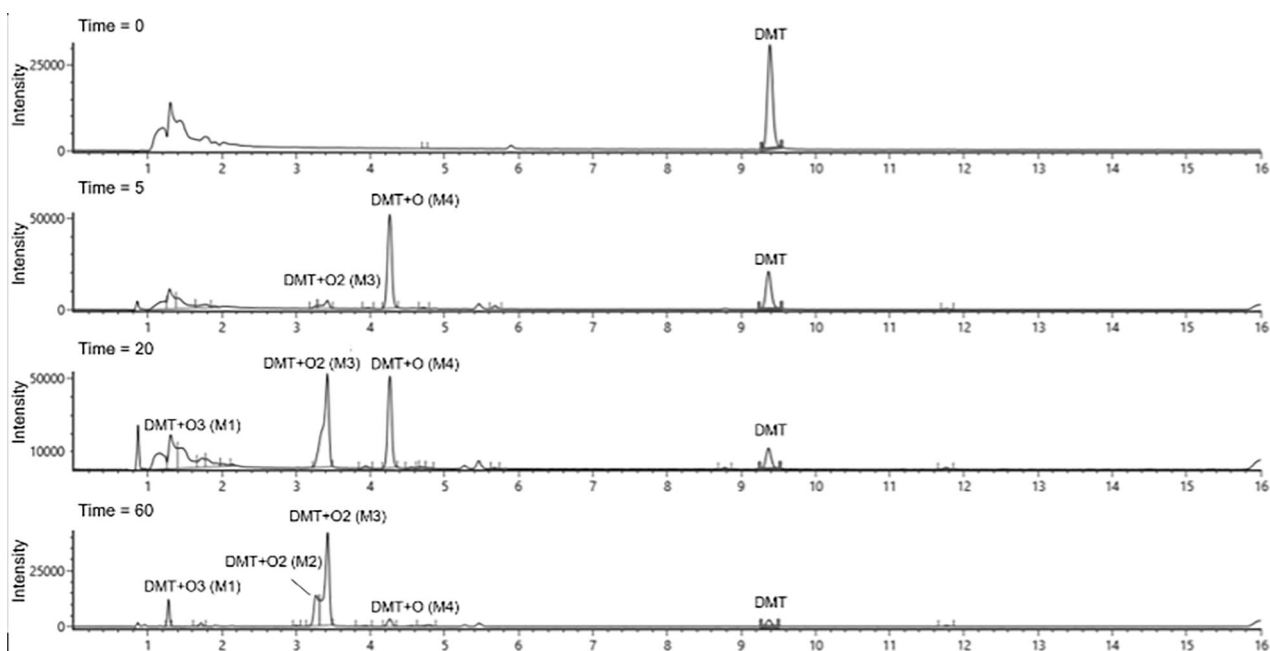


Figure 1. Combined extracted chromatogram of detected metabolites at different time points after incubation of DMT with CYP2D6.

At later time points, the M4 peak was reduced and the tri-oxygenated metabolite M1 as well as the di-oxygenated metabolites M2 and M3 appeared. This indicates a sequential metabolism with M1, M2 and M3 being formed from M4. In addition, some of the metabolites had slightly shifting retention times when re-injected (data not shown). As quality controls and system suitability tests were run daily without indicating any chromatographic problems, and as it was only the retention time of some metabolites and not DMT that shifted, this would indicate chemical instability. Individual chromatograms of the major metabolites are provided in the [Supplementary information](#) (Figures S1-S3). The response of each metabolite over time is presented in [Figure 2](#). Some minor metabolites were also detected, including NMT, DMT *N*-oxide, psilocin and bufotenine. However, the peak areas of these metabolites were substantially smaller than for M1-M4. No metabolites were detected using HR-MS after incubation with HLM.

M4 eluted at 4.26 min with a molecular shift of +15.9873 Da from DMT, indicating oxygenation. M4 had a fragmentation pattern similar to DMT with the metabolic transformation on fragments 160 and 132 ([Figure 3](#) and [Figure S8](#)), indicating hydroxylation on the indole core. As injected reference standards of psilocin (4-OH) and bufotenine (5-OH) had different retention times than M4, hydroxylation at the 4- and 5-position can be excluded, leading to the conclusion that 6-OH-DMT or 7-OH-DMT are the most likely metabolites formed in these experiments. Alternatively, hydroxylation at the 2-position and subsequent keto-enol tautomerism to the corresponding ketone could also occur. At the same retention time as M4 and with an exactly overlapping chromatographic peak profile, a peak with a mass shift of +2 O (+31.9819 Da) compared to DMT was detected. A similar phenomenon was observed for the psilocin and bufotenine reference standards with observed peaks corresponding to  $a+2O$  mass shift appearing at the same

retention times. Consequently, it was concluded that this was likely due to in source adduct formation, i.e. the result of a chemical reaction in the MS electrospray source. Therefore, the +O2 peak observed at 4.26 min in the incubation mixtures from DMT was not considered to be an actual metabolite.

M2 and M3 had retention times of 3.25 and 3.42 min respectively with  $a+31.9819$  Da shift from DMT, corresponding to the molecular weight of two oxygen atoms. Their fragmentation pattern suggests that the metabolic transformation has occurred on the indole core ([Figure 3](#) and [Figures S6](#) and [S7](#)). The molecular structures of M2 and M3 cannot be elucidated from these experiments but a possible explanation is the formation of diols *via* hydroxylation of M4.

M1 had a retention time of 1.30 min and  $a+47.9780$  Da shift from DMT, corresponding to three oxygen atoms. The fragmentation pattern again suggests that the oxidation has occurred at the indole core as fragment of  $m/z$  58 (corresponding to an unchanged dimethylamine substituent on the side chain) and  $m/z$  164 (corresponding to the indole core +3O) were observed ([Figure 3](#) and [Figure S5](#)). In addition, as M1 appeared at later time points while M2 and M3 decreased over time, indicating a stepwise metabolism, it seems likely that M1 might be formed from M2 and M3, meaning that at least two of the oxygenations have occurred on the indole core. A suggested metabolic pathway of DMT *via* CYP2D6 is presented in [Figure 4](#).

## Discussion

This work aimed to investigate the involvement of CYP enzymes in the metabolism of DMT as well as to identify which metabolites are formed *via* these enzymes.

After incubation with a battery of recombinant CYP enzymes, DMT was shown to be a substrate for CYP2D6 while no DMT depletion was observed with any of the other

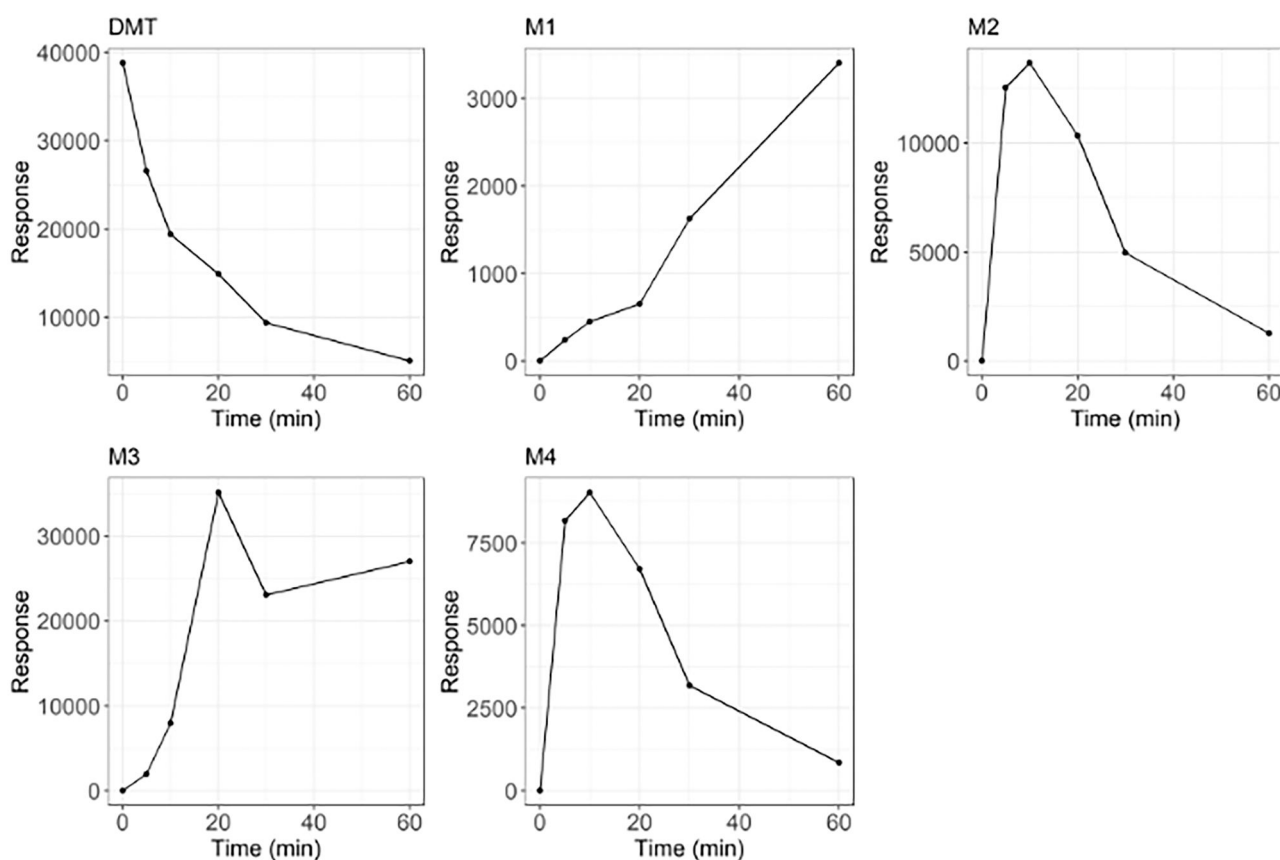


Figure 2. Signal response of DMT and the four major metabolites over time after incubation of DMT with CYP2D6.

investigated isozymes. These findings support a newly published paper by Good et al. (Good et al. 2023) which showed that DMT is a substrate for CYP2D6, although they also reported a minor role for CYP2C19. Admittedly, no positive controls were used in the present study and it is possible that this discrepancy could be explained by failed experiments with CYP2C19 in our case. Nevertheless, the reported CYP2C19 activity was substantially lower than that of CYP2D6 and with the combined results of this study and the aforementioned study by Good et al. it is likely that CYP2D6 is indeed the most relevant enzyme for the CYP-mediated metabolism of DMT. CYP2D6 has also been shown capable of metabolising several similar psychoactive tryptamine derivatives (Michely et al. 2015; 2017; Caspar et al. 2018). The results of our experiments further confirm a potential role for CYP2D6 in DMT metabolism. However, as metabolism by MAO-A is the major metabolic pathway *in vivo*, the importance of CYP2D6 metabolism is likely minor after administration of DMT alone. Nevertheless, as CYP2D6 is a known polymorphic enzyme (Taylor et al. 2020) as well as a subject for inhibition by several common therapeutic drugs (Crewe et al. 1992), this metabolic pathway warrants further investigation to ensure safe and efficacious administration of DMT in the future, especially when taken together with MAO-inhibitors.

DMT was also observed to be rapidly metabolised in HLM with substantial amounts of IAA forming. HLM are subcellular fractions derived from the endoplasmic reticulum of hepatocytes. While MAO-A is mainly bound to the mitochondrial

membrane in cells, smaller amounts of microsomal MAO have also been reported (Tipton 1986). It is clear from the rapid formation of IAA in our experiments that some MAO-A was indeed present, making it difficult to study CYP mediated metabolism in isolation using HLM. This could be due to intrinsic microsomal MAO-A but it is also possible that HLM contains traces of cytosolic MAO-A. Harmine, which is one of the main constituents of ayahuasca, significantly reduced DMT metabolism in HLM. Harmine is known to be an inhibitor of both MAO-A and CYP2D6 (Zhao et al. 2011), and the large reduction in metabolic rate of DMT in the HLM incubations with harmine is likely explained by inhibition of these enzymes. However, as these incubations were not analysed for CYP2D6-specific metabolites, we cannot say if complete inhibition of CYP2D6 occurred at these concentrations. After incubation with quinidine, no reduction in metabolic rate was observed, likely explained by the rapid metabolism of DMT *via* MAO-A. Interestingly, the general CYP inhibitor SKF-525A had a larger impact on metabolic rate than quinidine, which would indicate the involvement of additional CYP enzymes in the metabolism of DMT or inhibition of MAO-A by SKF-525A.

Subsequent analysis of samples generated by incubation of DMT with CYP2D6 resulted in the proposed metabolic pathway presented in Figure 4. Interestingly, similar metabolic pathways have been suggested for several other dialkylated tryptamines. Mono-, di- and tri-hydroxylation have been reported to occur on the indole core of *N*, *N*-diallyltryptamine, 5-methoxy-*N*, *N*-diallyltryptamine and 5-fluoro-

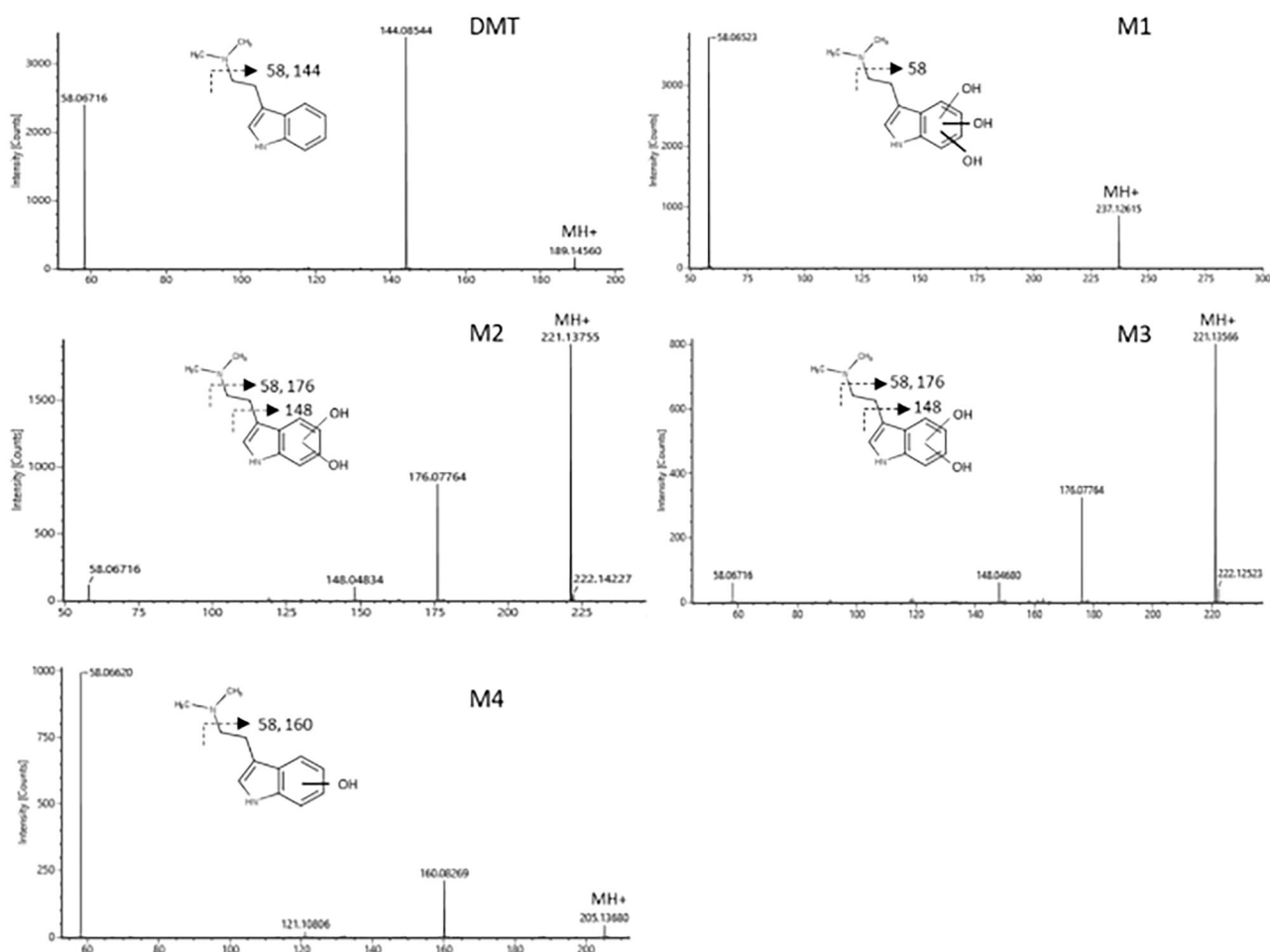


Figure 3. Fragmentation patterns of DMT and the identified metabolites at a collision energy of 10 eV.

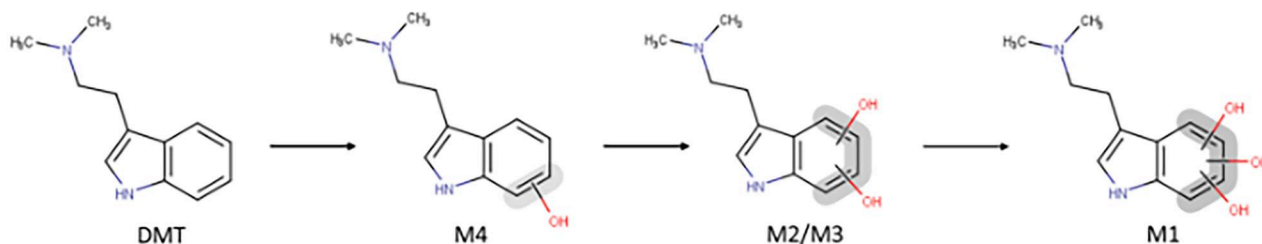


Figure 4. Proposed metabolic pathway of DMT via CYP2D6.

diallyltryptamine (Michely et al. 2015; 2017). Mono- and/or di-hydroxylation on the indole core has also been reported for 7-methyl-diallyltryptamine, 5,6-methylenedioxy-diallyltryptamine, 5-methoxy-*N,N*-diisopropyltryptamine, *N*-ethyl-*N*-propyltryptamine,  $\alpha$ -methyltryptamine and *O*-acetylpsilocin (Kamata et al. 2006; Michely et al. 2017; Manier et al. 2021; Malaca et al. 2023). However, in contrast to most previously published studies, we detected only one mono-hydroxylated metabolite in any significant amounts in our study. Albeit not likely, as a very flat chromatographic gradient was used, it cannot be excluded that the peak observed may consist of two or more co-eluting isobaric metabolites. In addition to the reports on other tryptamine derivatives, 7-OH-DMT has previously been reported as a potential metabolite of DMT (Szara and Axelrod 1959).

DMT has also been shown to be a substrate for peroxidases leading to formation of di-oxidated metabolites with the same molecular mass as M2 and M3 reported here (Gomes et al. 2014). The authors suggested that these would result from an opening of the indole-ring. However, since the fragmentation pattern of M2 and M3 is very similar to that of DMT, it seems unlikely that a ring opening has occurred. Nevertheless, as the MSMS spectra do not give sufficient information regarding the exact position of the transformations, further studies are needed to confirm their identity. Furthermore, as both the 4- and 5-hydroxylated versions of DMT (psilocin and bufotenine) are psychoactive, any potential role of the proposed metabolites in the psychoactive effects of DMT should be further investigated. On the

assumption that the CYP2D6 metabolites are active and that MAO-inhibitors would significantly shift DMT metabolic pathways, it is conceivable that this could partly explain any differences in subjective experiences after administration of intravenous or smoked DMT compared to that of ayahuasca.

None of the M1-M4 metabolites were detected with HR-MS after incubation of DMT with HLM. However, as already mentioned, the formation of IAA was confirmed using a quantitative LC-MS/MS method indicating the presence of MAO-A in these experiments. The failure to detect any of the M1-M4 metabolites in these experiments indicates that CYP2D6 may be of minor importance when MAO-A is present.

To conclude, the current study confirms the involvement of CYP2D6 in the metabolism of DMT. Furthermore, CYP2D6 metabolism likely leads to hydroxylation on the indole core, resulting in mono-, di- and tri-hydroxylated metabolites. While the role of this metabolic pathway *in vivo* may be of minor importance when DMT is administered as monotherapy, this could change after concomitant intake of MAO inhibitors. The results of this study indicate that more research is needed on the metabolic pathways of DMT to understand any potential risk for short-term drug-drug interactions, especially following ayahuasca intake. As CYP2D6 is a polymorphic enzyme, the potential impact of being a poor metabolizer with regards to CYP2D6 also needs to be taken into consideration. Further research to investigate the molecular structures of the proposed metabolites and to understand if they could contribute to the psychoactive effects of DMT administration when combined with MAO inhibitors is needed.

## Acknowledgements

The authors thank Fanny Höglund for her assistance with the HLM experiments and Clinical Chemistry at Sahlgrenska University Hospital for letting us use their LC-HRMS instrumentation.

## Disclosure statement

The authors report there are no competing interests to declare.

## Funding

The author(s) reported there is no funding associated with the work featured in this article.

## References

- Buckholtz NS, Boggan WO. 1977. Monoamine oxidase inhibition in brain and liver produced by beta-carbolines: structure-activity relationships and substrate specificity. *Biochem Pharmacol.* 26(21):1991–1996. doi:10.1016/0006-2952(77)90007-7.
- Caspar AT, Gaab JB, Michely JA, Brandt SD, Meyer MR, Maurer HH. 2018. Metabolism of the tryptamine-derived new psychoactive substances 5-MeO-2-Me-DALT, 5-MeO-2-Me-ALCHT, and 5-MeO-2-Me-DIPT and their detectability in urine studied by GC-MS, LC-MS(n), and LC-HR-MS/MS. *Drug Test Anal.* 10(1):184–195. doi:10.1002/dta.2197.
- Crewe HK, Lennard MS, Tucker GT, Woods FR, Haddock RE. 1992. The effect of selective serotonin re-uptake inhibitors on cytochrome P4502D6 (CYP2D6) activity in human liver microsomes. *Br J Clin Pharmacol.* 34(3):262–265. doi:10.1111/j.1365-2125.1992.tb04134.x.
- D'Souza DC, Syed SA, Flynn LT, Safi-Aghdam H, Cozzi NV, Ranganathan M. 2022. Exploratory study of the dose-related safety, tolerability, and efficacy of dimethyltryptamine (DMT) in healthy volunteers and major depressive disorder. *Neuropsychopharmacology.* 47(10):1854–1862. doi:10.1038/s41386-022-01344-y.
- Dobkin de Rios M. 1971. Ayahuasca—the healing vine. *Int J Soc Psychiatry.* 17(4):256–269. doi:10.1177/002076407101700402.
- Eckernäs E, Bendrioua A, Cancellarini C, Timmermann C, Carhart-Harris R, Hoffmann KJ, Ashton M. 2022. Development and application of a highly sensitive LC-MS/MS method for simultaneous quantification of N, N-dimethyltryptamine and two of its metabolites in human plasma. *J Pharm Biomed Anal.* 212:114642. doi:10.1016/j.jpba.2022.114642.
- Food and Drug Administration 2020. *In Vitro Drug Interaction Studies—Cytochrome P450 Enzyme- and Transporter-Mediated Drug Interactions Guidance for Industry.* WA: US department of Health and Human Services FDA.
- Gomes MM, Coimbra JB, Clara RO, Dörr FA, Moreno AC, Chagas JR, Tufik S, Pinto E, Jr., Catalani LH, Campa A. 2014. Biosynthesis of N, N-dimethyltryptamine (DMT) in a melanoma cell line and its metabolization by peroxidases. *Biochem Pharmacol.* 88(3):393–401. doi:10.1016/j.bcp.2014.01.035.
- Good M, Joel Z, Benway T, Routledge C, Timmermann C, Erritzoe D, Weaver R, Allen G, Hughes C, Topping H, et al. 2023. Pharmacokinetics of N, N-dimethyltryptamine in Humans. *Eur J Drug Metab Pharmacokinet.* 48(3):311–327. doi:10.1007/s13318-023-00822-y.
- Kamata T, Katagi M, Kamata HT, Miki A, Shima N, Zaitso K, Nishikawa M, Tanaka E, Honda K, Tsuchihashi H. 2006. Metabolism of the psychotomimetic tryptamine derivative 5-methoxy-N, N-diisopropyltryptamine in humans: identification and quantification of its urinary metabolites. *Drug Metab Dispos.* 34(2):281–287. doi:10.1124/dmd.105.005835.
- Luethi D, Kolaczynska KE, Vogt SB, Ley L, Erne L, Liechti ME, Duthaler U. 2022. Liquid chromatography-tandem mass spectrometry method for the bioanalysis of N, N-dimethyltryptamine (DMT) and its metabolites DMT-N-oxide and indole-3-acetic acid in human plasma. *J Chromatogr B Analyt Technol Biomed Life Sci.* 1213:123534. doi:10.1016/j.jchromb.2022.123534.
- Malaca S, Bottinelli C, Fanton L, Cartiser N, Carlier J, Busardò FP. 2023.  $\alpha$ -Methyltryptamine ( $\alpha$ -MT) Metabolite Profiling in Human Hepatocyte Incubations and Postmortem Urine and Blood. *Metabolites.* 13(1):92. doi:10.3390/metabo13010092.
- Manier SK, Felske C, Zapp J, Eckstein N, Meyer MR. 2021. Studies on the In Vitro and In Vivo Metabolic Fate of the New Psychoactive Substance N-Ethyl-N-Propyltryptamine for Analytical Purposes. *J Anal Toxicol.* 45(2):195–202. doi:10.1093/jat/bkaa060.
- McIlhenny EH, Riba J, Barbanoj MJ, Strassman R, Barker SA. 2012. Methodology for determining major constituents of ayahuasca and their metabolites in blood. *Biomed Chromatogr.* 26(3):301–313. doi:10.1002/bmc.1657.
- Michely JA, Brandt SD, Meyer MR, Maurer HH. 2017. Biotransformation and detectability of the new psychoactive substances N, N-diallyltryptamine (DALT) derivatives 5-fluoro-DALT, 7-methyl-DALT, and 5,6-methylene-dioxy-DALT in urine using GC-MS, LC-MS(n), and LC-HR-MS/MS. *Anal Bioanal Chem.* 409(6):1681–1695. doi:10.1007/s00216-016-0117-5.
- Michely JA, Helfer AG, Brandt SD, Meyer MR, Maurer HH. 2015. Metabolism of the new psychoactive substances N, N-diallyltryptamine (DALT) and 5-methoxy-DALT and their detectability in urine by GC-MS, LC-MSn, and LC-HR-MS-MS. *Anal Bioanal Chem.* 407(25):7831–7842. doi:10.1007/s00216-015-8955-0.
- Palhano-Fontes F, Barreto D, Onias H, Andrade KC, Novaes MM, Pessoa JA, Mota-Rolim SA, Osório FL, Sanches R, Dos Santos RG, et al. 2019. Rapid antidepressant effects of the psychedelic ayahuasca in treatment-resistant depression: a randomized placebo-controlled trial. *Psychol Med.* 49(4):655–663. doi:10.1017/S0033291718001356.



- Riba J, McIlhenny EH, Bouso JC, Barker SA. 2015. Metabolism and urinary disposition of N, N-dimethyltryptamine after oral and smoked administration: a comparative study. *Drug Test Anal.* 7(5):401–406. doi:10.1002/dta.1685.
- Riba J, McIlhenny EH, Valle M, Bouso JC, Barker SA. 2012. Metabolism and disposition of N, N-dimethyltryptamine and harmala alkaloids after oral administration of ayahuasca. *Drug Test Anal.* 4(7-8):610–616. doi:10.1002/dta.1344.
- Sanches RF, de Lima Osório F, Dos Santos RG, Macedo LR, Maia-de-Oliveira JP, Wichert-Ana L, de Araujo DB, Riba J, Crippa JA, Hallak JE. 2016. Antidepressant Effects of a Single Dose of Ayahuasca in Patients With Recurrent Depression: A SPECT Study. *J Clin Psychopharmacol.* 36(1):77–81. doi:10.1097/JCP.0000000000000436.
- Szara S, Axelrod J. 1959. Hydroxylation and N-demethylation of N, N-dimethyltryptamine. *Experientia.* 15(6):216–217. doi:10.1007/BF02158111.
- Taylor C, Crosby I, Yip V, Maguire P, Pirmohamed M, Turner RM. 2020. A Review of the Important Role of CYP2D6 in Pharmacogenomics. *Genes (Basel).* 11(11):1295. doi:10.3390/genes11111295.
- Tipton KF. 1986. Enzymology of monoamine oxidase. *Cell Biochem Funct.* 4(2):79–87. doi:10.1002/cbf.290040202.
- Vogt SB, Ley L, Erne L, Straumann I, Becker AM, Klaiber A, Holze F, Vandersmissen A, Mueller L, Duthaler U, et al. 2023. Acute effects of intravenous DMT in a randomized placebo-controlled study in healthy participants. *Transl Psychiatry.* 13(1):172. doi:10.1038/s41398-023-02477-4.
- Zhao T, He YQ, Wang J, Ding KM, Wang CH, Wang ZT. 2011. Inhibition of human cytochrome P450 enzymes 3A4 and 2D6 by  $\beta$ -carboline alkaloids, harmine derivatives. *Phytother Res.* 25(11):1671–1677. doi:10.1002/ptr.3458.